Journal of Magnetism and Magnetic Materials 473 (2019) 61–67

Contents lists available at ScienceDirect

Journal of Magnetism and Magnetic Materials

journal homepage: www.elsevier.com/locate/jmmm

Research articles

Functionalization of T lymphocytes for magnetically controlled immune therapy: Selection of suitable superparamagnetic iron oxide nanoparticles

Marina Mühlberger[a], Christina Janko[a], Harald Unterweger[a], Eveline Schreiber[a], Julia Band[a], Christian Lehmann[b], Diana Dudziak[b], Geoffrey Lee[c], Christoph Alexiou[a], Rainer Tietze[a,*]

[a] Department of Otorhinolaryngology, Head and Neck Surgery, Section of Experimental Oncology and Nanomedicine (SEON), Else Kröner-Fresenius-Stiftung-Professorship, Universitätsklinikum Erlangen, Erlangen, Germany
[b] Department of Dermatology, Laboratory of Dendritic Cell Biology, Universitätsklinikum Erlangen, Erlangen, Germany
[c] Division of Pharmaceutics, Friedrich-Alexander-Universität Erlangen-Nürnberg, Erlangen, Germany

ARTICLE INFO

Keywords:
Superparamagnetic iron oxide nanoparticle
T lymphocyte
Immune therapy
Cancer
Solid tumor
Magnetic targeting

ABSTRACT

According to the World Health Organization, cancer is the second most important cause of death in Europe. Due to its manifold manifestations, it is not possible to treat all patients according to a uniform scheme. However, all solid tumors have one thing in common: independent of the tumor's molecular subgroup and the treatment protocol, the immune status of the tumor, especially the amount of tumor infiltrating lymphocytes (TILs), is important for the patient's clinical outcome – the higher the number of TILs, the better the outcome. For this reason it seems desirable to increase the number of TILs.

One way to accumulate T cells in the tumor area is to make them magnetizable and attract them with an external magnetic field. Magnetization can be achieved by superparamagnetic iron oxide nanoparticles (SPIONs) which can be bound to the cells' surface or internalized into the cells.

For this study, SPIONs with different coatings were synthesized and incubated with immortalized mouse T lymphocytes. SPIONs only stabilized with lauric acid (LA) coated *in situ* or afterwards showed high toxicity. Addition of an albumin layer increased the biocompatibility but reduced cellular uptake. To increase the cellular uptake the albumin coated particles were aminated, leading to both higher uptake and toxicity, dependent on the degree of amination. In the presence of an externally applied magnetic field, T cells loaded with selected types and amounts of SPIONs were guidable.

With this promising pilot study we already can demonstrate that it is possible to attract SPION bearing T cells by an external magnet.

To sum up, biocompatibility and uptake of SPIONs by T cells are opposing events. Thus, for the functionalization of T cells with SPIONs the balance between uptake and toxicity must be evaluated carefully.

1. Introduction

In 2012, cancer was the cause for 13% of cases of death worldwide [1]. The development and progression of cancer is a dynamic biological and evolutionary process. It involves a composite organ system with transcriptome shaped by gene aberrations, epigenetic changes, the cellular biological context and environmental influences. Solid cancer growth and response to treatment has a number of characteristics that are specific to the individual patient, examples of which are the tumor's molecular subgroup or the interaction with neighboring tissue. In contrast, the immune status of the solid tumor is universally important [2]. The prognosis of patients suffering from solid tumors (such as melanoma, breast, lung or colorectal cancer) has been demonstrated to be much better when primary tumors already displayed an anti-tumor

Abbreviations: AES, atomic emission spectroscopy; AxV, annexin A5 FITC conjugate; BSA, bovine serum albumin; DiI, $DiIC_1(5)$ (1,1′-dimethyl-3,3,3′,3′-tetramethylindodicarbocyanine iodide); DLS, dynamic light scattering; DMEM, Dulbecco's modified Eagle's medium; EDA, ethylenediamine; EDC, 1-ethyl-3-(3-dimethylaminopropyl)carbodiimide; FCS, fetal calf serum; FITC, fluorescein isothiocyanate; FT-IR, Fourier-transform infrared spectroscopy; Hoe, Hoechst 33342; LA, lauric acid; LY, Lucifer Yellow; MDT, magnetic drug targeting; MRI, magnetic resonance imaging; MTcT, magnetic T cell targeting; PBS, phosphate buffered saline; PI, propidium iodide; SPION, superparamagnetic iron oxide nanoparticle; SSc, side scatter; TIL, tumor infiltrating lymphocyte

* Corresponding author at: Section of Experimental Oncology and Nanomedicine, ENT Department, Universitätsklinikum Erlangen, Glückstr. 10a, 91054 Erlangen, Germany.
E-mail address: rainer.tietze@uk-erlangen.de (R. Tietze).

https://doi.org/10.1016/j.jmmm.2018.10.022
Received 21 June 2018; Received in revised form 4 October 2018; Accepted 4 October 2018
Available online 05 October 2018
0304-8853/

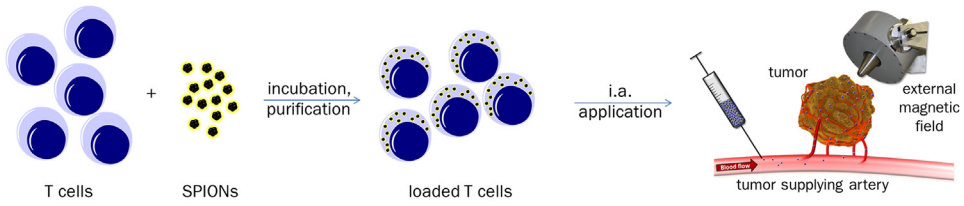

Fig. 1. Concept of Magnetic T cell Targeting. T cells are incubated with SPIONs, purified and applied into a tumor supplying artery while an external magnetic field is present in the tumor area. The loaded T cells are attracted by the magnetic field and accumulate in the tumor area as tumor infiltrating lymphocytes.

immune signature. This means that the presence of tumor infiltrating lymphocytes (TILs), especially $CD8^+$ cytotoxic T cells, in the tumor area was directly correlated with the clinical outcome of the patient, which was independent on the treatment protocol [3,4]. For this reason it seems desirable to increase the number of TILs supplementary to the individual treatment protocol.

Besides the use of bispecific antibodies as for example described by Frankel et al. [5], a way to accumulate T cells in the tumor area is to make them magnetizable and attract them with an external magnetic field (Fig. 1). This method offers some advantages: on the one hand, no bispecific antibodies are required to bind the T cells in the tumor area. The use of a bispecific antibody is associated with high costs and is very specific, as each tumor and T cell type would need its own antibody, whereas magnetically controllable T cells can be used for any solid tumor or even for the better navigation of engineered CAR-T cells. On the other hand, the systemic distribution of T cells in the entire body is avoided by injection into a tumor supplying artery, so that not an extremely large number of T cells are required. Magnetization can be achieved by superparamagnetic iron oxide nanoparticles (SPIONs) which are bound to the cells' surfaces or internalized into the cells. Vaněček et al. has already used this type of cell control in mesenchymal stem cells to repair spinal cord injuries [6]. However, these two ways of magnetic cell targeting cannot be simply compared, as the type of application (intrathecal vs. intraarterial) and also the environmental conditions (cerebrospinal fluid, low pressure vs. blood, high pressure) differ fundamentally. Therefore, the aim of this study was to prove that it is possible to control and direct T cells magnetically analogous to magnetic drug targeting (MDT), an established method to bring drugs to the desired place by magnetic forces [7–9]. In addition, SPIONs can be used as contrast agents in magnetic resonance imaging or X-ray tomography so that the loaded T cells might be tracked as part of an imaging guided therapy [10,11].

But unlike labelling of T cells for MRI tracking as published by various working groups [12,13], the amount of SPION uptake for attracting and directing them by an external magnetic field has to be higher and the SPIONs have to have high susceptibility. For this reason, the combination of a particle system and incubation conditions with T cells has to be tested systematically.

2. Materials and methods

2.1. Materials

Iron (II) chloride tetrahydrate ($FeCl_2{\cdot}4H_2O$), iron (III) chloride hexahydrate ($FeCl_3{\cdot}6H_2O$), acetic acid (glacial) and bovine serum albumin fraction V (BSA) were purchased from Merck (Darmstadt, Germany). Heavy metal-free dialysis tubes Spectrapor 7 (MWCO 10 kDa) and tangential ultrafiltration columns (MWCO 100 kDa) were supplied by Spectrum Labs (Frankfurt, Germany), lauric acid (LA) by AppliChem (Darmstadt, Germany). Ammonium chloride, hydrochloric acid 25%, sodium hydroxide, nitric acid 65%, ammonia solution 25%, acetone, 2-propanol, ninhydrin, 1-ethyl-3-(3-dimethylaminopropyl) carbodiimide hydrochloride (EDC·HCl), ethylenediamine dihydrochloride (EDA·2HCl) and sodium acetate were purchased from Carl Roth (Karlsruhe, Germany). Vivaspin 20 ultrafiltration units (MWCO 100,000 Da) and Minisart NML syringe filters (0.8 µm and 0.2 µm pore size) were supplied by Sartorius (Goettingen, Germany). Annexin A5 FITC conjugate (AxV), Hoechst 33342 (Hoe), $DiIC_1(5)$ (1,1′-dimethyl-3,3,3′,3′-tetramethylindodicarbocyanine iodide, DiI), GlutaMAX supplement and penicillin streptomycin-solution 5000 U/mL were purchased from Thermo Fisher Scientific (Waltham, MA, USA), Ringer's solution from Fresenius Kabi (Bad Homburg, Germany). Dulbecco's modified Eagle's medium (DMEM) and fetal calf serum (FCS) were supplied by Biochrom (Berlin, Germany), propidium iodide (PI), Lucifer Yellow CH dipotassium salt (LY), 2-methoxyethanol, hydrindantin dihydrate and phosphate-buffered saline (PBS) by Sigma-Aldrich (Taufkirchen, Germany). The water used in all experiments was purified by means of a Siemens Ultra Clear system (Evoqua Water Technologies, Günzburg, Germany).

2.2. Nanoparticle synthesis

The LA particles, consisting of a multi core iron oxide center and chelate bound lauric acid coating (Fig. 2①), were synthesized by alkaline coprecipitation and subsequent coating with lauric acid as described by Tietze et al. [14]. Briefly, iron (II) chloride and iron (III) chloride salts in a molar ratio of 2:3 were solved in water. While stirring, 25% ammonia solution (half of the water volume) was added to precipitate iron oxide particles. After 30 min, the particles were washed magnetically with 1.3% ammonia solution until the supernatant was free of chloride. The washed particles were re-suspended in 1.3% ammonia solution. The required amount of this suspension was mixed with lauric acid and heated to 90 °C while stirring. After cooling to room

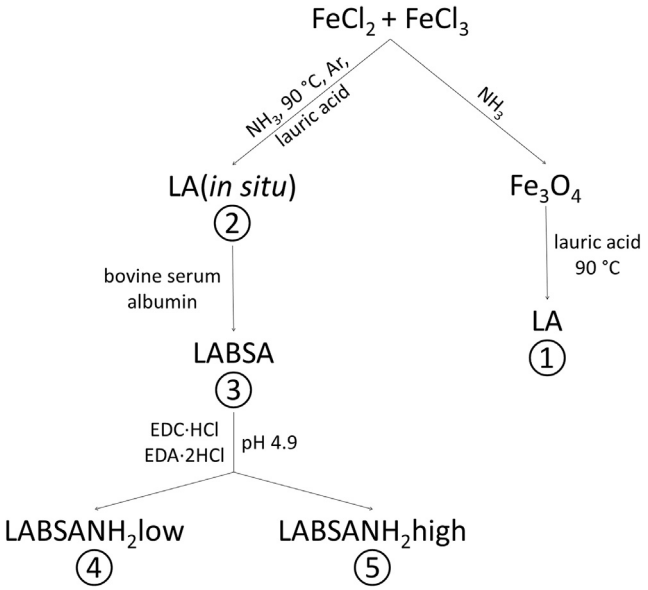

Fig. 2. Synthesis overview. All SPIONs used were synthesized by alkaline coprecipitation.

temperature the suspension was diluted with water to its 8.5 fold volume and filtered through 0.8 µm and sterile 0.2 µm syringe filters.

The LA(*in situ*) particles, also consisting of a multi core iron oxide center, but coated with lauric acid *in situ* (Fig. 2②), and LABSA particles, which are LA(*in situ*) particles coated with adsorptive bound bovine serum albumin (BSA) (Fig. 2③), were both produced by alkaline precipitation with *in situ* coating according to a protocol of Zaloga et al. [15]. In brief, iron (II) chloride and iron (III) chloride salts were dissolved in water in a molar ratio of 1:2 and stirred under an argon atmosphere at 90 °C. The same volume of 25% ammonia solution was added followed by lauric acid dissolved in acetone. After 15 min of homogenizing and another 15 min of cooling to room temperature the same amount of water as in the beginning was added. The suspension was filtered through 0.8 µm syringe filters into dialysis tubes with a MWCO of 10 kDa and dialyzed multiple times. The purified LA(*in situ*) particles were diluted to the fivefold of the starting volume and the pH was adjusted to 9.0.

The required amount of LA(*in situ*) for a concentration of 2.5 mg/mL iron was added dropwise through a 0.8 µm syringe filter under stirring to the required amount of 20% BSA stock solution, filtered through a 0.2 µm syringe filter, for a concentration of 6% BSA (wt./vol%) and diluted with water. After 5 min of stirring, the suspension was ultrafiltrated using Vivaspin 20 ultrafiltration units (MWCO 100 kDa, 6,500x g) in a 5430 Eppendorf centrifuge (Hamburg, Germany) to concentrate the volume to half of the reaction volume. The LABSA particles were sterile filtered through 0.2 µm syringe filters.

$LABSANH_2$ particles, being aminated LABSA particles (Fig. 2④ + ⑤), were synthesized by amination of LABSA particles according to a method for aqueous media by Nakajima et al. [16]. EDC·HCl was used as coupling reagent and EDA·2HCl as primary amine.

For the higher amination degree 9 mmol EDA and 0.78 mmol EDC were dissolved in water, adjusted to pH 4.9 and added to the volume of LABSA corresponding to 25 mg iron. The pH value was adjusted to 4.9 again and the mixture stirred for 180 min. The reaction was stopped by adding sodium acetate buffer. The suspension was ultracentrifugated in Vivaspin 20 ultracentrifugation units (MWCO 100 kDa, 6500x g) and washed with water at least five times. Purification of excess EDA was controlled by FT-IR spectra of lyophilized samples using a Bruker Alpha FTIR spectrometer (Bruker, Billerica, MA, USA) (see Supplementary Data S1). Sterile filtration was done through 0.2 µm syringe filters. For lower amination degree 0.9 mmol EDA and 0.078 mmol EDC were used. The other conditions correspond to those described above.

The synthesis procedure is summarized in Fig. 2.

2.3. Nanoparticle characterization

Iron concentrations were measured with microwave plasma atomic emission spectroscopy (AES) using an Agilent 4200 MP-AES (Agilent Technologies, Santa Clara, CA, USA).

Particles size was determined as hydrodynamic diameter by dynamic light scattering (DLS) with a Zetasizer Nano ZS (Malvern Panalytical, Almelo, Netherlands) at 25 °C in water (refractive index 1.33, viscosity 0.8872 cP) and cell culture medium (refractive index 1.335, viscosity 1.1100 cP, DMEM supplemented with 10% fetal calf serum (FCS), 1% L-glutamine and 1% penicillin streptomycin-solution).

The aqueous zeta potential was determined using a Zetasizer Nano ZS (Malvern Panalytical, Almelo, Netherlands) (25 °C, refractive index 1.33, viscosity 0.8872 cP, dielectric constant 78.5).

Susceptibility values as an indicator for magnetizability of the particles were acquired with a MS2G magnetic susceptibility meter (Bartington Instruments, Oxfordshire, UK) and are related to an iron concentration of 1 mg/mL as previously described by Unterweger et al. [10].

The degree of amination of the aminated LABSA particles was examined colorimetrically with ninhydrin and hydrindantin at 570 nm using a Biochrom Libra S22 UV/Vis spectrophotometer (Biochrom Ltd, Cambridge, UK). Ethylenediamine dihydochloride served as the external standard for the calibration curve. Since the brown-black particle suspension would interfere with the colorimetric determination, 6% BSA solution was used instead of the particles, which was aminated and purified in both degrees as described.

All measurements were done in triplicates.

2.4. Cell culture

The non-adherent T cell lines EL4 (ATCC TIB-39) and BW5147.3 (ATCC TIB-47), both from mouse lymphoma, were cultured in DMEM supplemented with 10% fetal calf serum, 1% L-glutamine and 1% penicillin streptomycin-solution 5000 U/mL at 37 °C at humidified 5% CO_2 atmosphere. The cells were passaged twice a week. To determine cell count and viability, MUSE Cell Analyzer (Merck, Darmstadt, Germany) was used.

2.5. Flow cytometry

Effects of potential particle toxicity on cell viability were examined by flow cytometry. $5x10^4$ cells were seeded in 1 mL medium in triplicates in 24-well plates and incubated with various concentrations of SPIONs for 24 and 48 h. After incubation, cells were stained with a mixture containing 1 µL/mL Hoechst (10 mg/mL), 2 µL/mL AxV, 2 µL/mL PI (0.33 mg/mL) and 0.4 µL/mL DiI (10 µM) in Ringer's solution. Hoechst was used to mark cells as such by staining the cell nucleus, AxV and PI for the detection of apoptotic and necrotic cells and DiI additionally for the determination of the mitochondrial membrane integrity. Fluorescence was measured with a Gallios flow cytometer and analyzed with Kaluza 1.2 Analysis Software (Beckman Coulter Life Sciences, Indianapolis, IN, USA).

Since the internalization of SPIONs alters the granularity of the cells, the side scatter (SSc) was used to estimate and compare the uptake of nanoparticles into the cells [17].

In addition, staining with the fluorescent membrane-impermeable dye Lucifer Yellow (LY), which gets coingested by cells with particle uptake, was performed to estimate whether the particles were internalized into the cells or adsorbed to the cell surface. 5×10^4 cells were seeded in 1 mL medium in triplicates in 24-well plates and incubated with 2 µg/mL LY and various concentrations of SPIONs for 24 and 48 h. After incubation, cells were stained with a mixture containing 1 µL/mL Hoechst (10 mg/mL), 2 µL/mL PI (0.33 mg/mL) and 0.4 µL/mL DiI (10 µM) in Ringer s solution and measured as described above.

All experiments were performed in at least two independent experiments in triplicates.

2.6. Uptake

The average particle uptake was determined as pg iron per cell. $2.5x10^5$ cells were seeded in 5 mL medium in triplicates in 6-well plates and incubated with various concentrations of SPIONs for 24 and 48 h. After incubation, cells were counted with the MUSE Cell Analyzer, washed twice with PBS and dried as pellet. For AES measurement the pellet was lysed with HNO_3 65% at 95 °C and diluted with water.

All experiments were performed in at least two independent experiments in triplicates.

2.7. Determination of magnetizability

To prove the concept of magnetic T cell targeting, videos were produced using an Axio Observer Z.1 microscope (Carl Zeiss, Oberkochen, Germany). $2.5x10^5$ cells were seeded in 6-well plates in 5 mL medium and incubated with various concentrations of SPIONs for 24 and 48 h. After incubation, cells were washed with PBS and re-suspended in fresh cell culture medium. From each sample 1 mL was transferred to a 24-well plate placed under the microscope. 60 s later, a

disc-shaped magnet (20 mm × 8 mm, approx. 200 mT) was placed in a neighboring well or a cylindrical magnet (8 mm × 5 mm, approx. 50 mT) was put in the same well and the cells' movement was filmed. To quantify the movement of cells, we used the software "Tracker Video Analysis and Modeling Tool" and measured the velocity of three fast moving cells in each video. All experiments were performed in at least two independent experiments.

2.8. Statistical analyses

For statistical analyses an unpaired Student's *t*-test in MS Excel was performed. A value of $p < 0.05$ was considered as statistically significant. In figures, statistical significance levels between control and treatment groups are represented by asterisks ($^{*}p < 0.05$; $^{**}p < 0.005$).

3. Results and discussion

3.1. Nanoparticle characterization

The hydrodynamic diameter of LA particles was 93.9 nm in water and 106.2 nm in DMEM + 10% FCS.

The *in situ* synthesis developed by Zaloga et al. [15] significantly reduced the hydrodynamic diameter of LA(*in situ*) particles to 40.3 nm in water (DMEM + 10% FCS: 80.5 nm). Coating with bovine serum albumin to improve biocompatibility increased the hydrodynamic particle diameter of LABSA particles to 81.7 nm in water (DMEM + 10% FCS: 43.9 nm). Aminating the BSA shell only led to a larger hydrodynamic diameter with a higher degree of amination. At low amination, the particles retained a hydrodynamic diameter of 81.5 nm in water (DMEM + 10% FCS: 43.3 nm), high amination led to 99.1 nm in water (DMEM + 10% FCS: 90.4 nm) (Fig. 3A).

The zeta potential also changed with the various coating steps (Fig. 3B). LA and LA(*in situ*) both had a negative zeta potential of −46.9 mV for LA and −34.8 mV for LA(*in situ*) in water due to the same coating substance. The surface potential of LABSA particles remained negative and was −34.9 mV. The amination of the protein coating increased the zeta potential of the particles, so that the weaker aminated LABSANH$_2$low reached an approximately neutral potential of −5.1 mV in water, while the more strongly aminated LABSANH$_2$high had +46.7 mV. The zeta potential of the particles in DMEM with 10% FCS was not measurable. All values obtained corresponded to those of the particle-free medium.

The values of susceptibility always refer to an iron concentration of 1 mg/mL. Since the *in situ* synthesis was carried out under protective gas and thus an oxidation of the particles during the synthesis was prevented, LA(*in situ*) reached a value of 7.9×10^{-3} instead of LA's 6.2×10^{-3}. After albumin coating, the susceptibility decreased to 6.2×10^{-3}. The reason for the decrease in susceptibility was on the one hand the ratio of shell to iron oxide core and the resulting lower number of iron oxide cores in the same sample volume, on the other hand oxidation as the protein coating was performed without protective gas. After amination, values of 5.6×10^{-3} for LABSANH$_2$low and 5.9×10^{-3} for LABSANH$_2$high were achieved (Fig. 3C). Since amination was also carried out without inert gas, the susceptibility is again reduced here.

In order to determine more precisely the differences in the degree of amination between LABSA, LABSANH$_2$low and LABSANH$_2$high, which are already shown by the increase in the zeta potential, amine residues of 6% BSA solution, 6% BSA solution low aminated (BSANH$_2$low) and 6% BSA solution high aminated (BSANH$_2$high) used as a substitute were quantified by means of a modified ninhydrin reaction [18]. In relation to pure BSA, BSANH$_2$low contains 9% more amine groups, BSANH$_2$high 147% more.

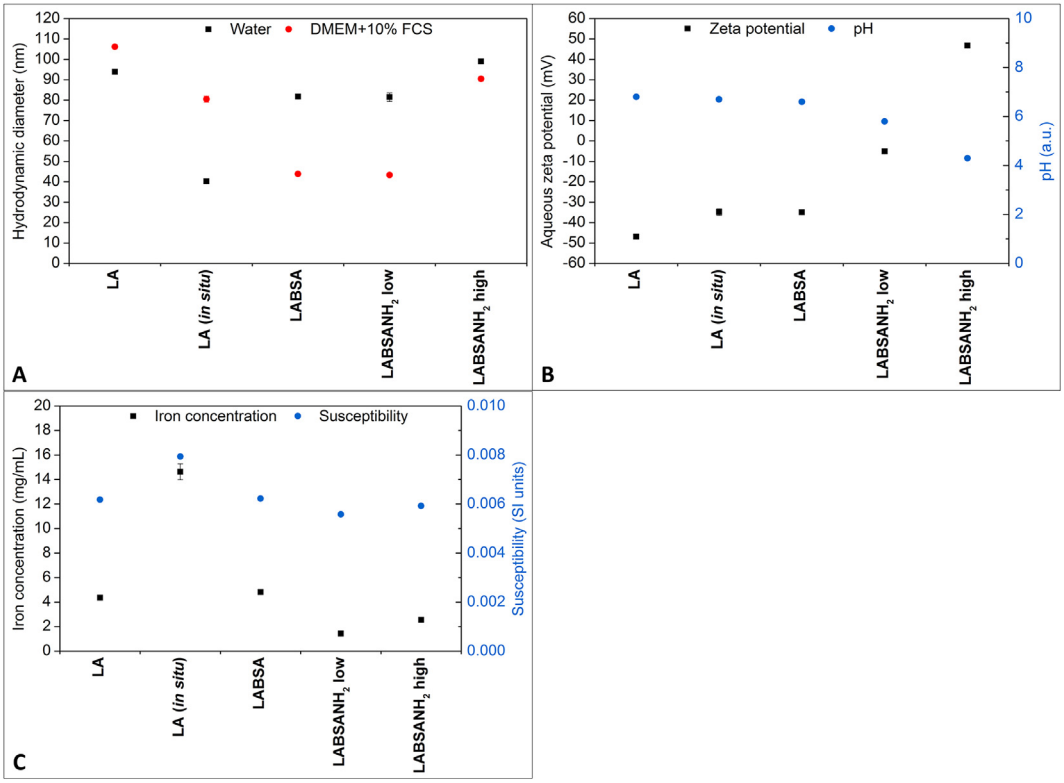

Fig. 3. Physicochemical characterization of the different SPIONs. A: *In situ* synthesis led to smaller hydrodynamic diameter. Coating with BSA and amination increased the size in water. B: Aqueous zeta potential shown in dependence of the pH value of the respective sample. C: Susceptibility (referred to an iron concentration of 1 mg/mL) was increased by the use of protective gas during the *in situ* synthesis.

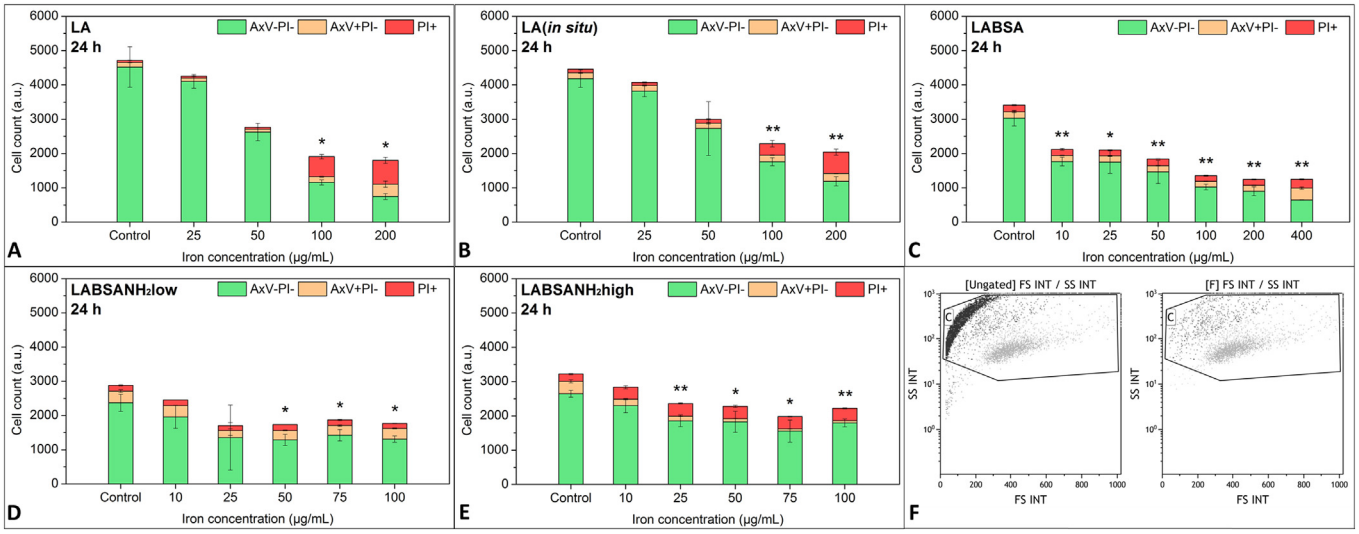

Fig. 4. Determination of relative cell count and biocompatibility by flow cytometry. A-E: Fluorescence staining with AxV and PI for detection of apoptotic (AxV + PI−) and necrotic (AxV + PI+) cells displayed as relative cell numbers to detect effects on cell proliferation. Shown are the mean values with standard deviations. F: Excess SPIONs (left) were removed from data analysis by gating on nucleated cells (Hoechst positive events) first (right). All experiments shown in this figure were performed with cell line BW5147.3. Student's *t*-test for AxV-PI- cells compared to control: $^{*}p < 0.05$, $^{**}p < 0.005$.

3.2. Toxicity

To find appropriate conditions for T cell loading, series of nanoparticle dilutions were investigated in the presence of BW5147.3 and EL4 cells. Cellular uptake and biocompatibility of the various nanoparticle systems were analyzed in flow cytometry after incubation for 24 or 48 h. Previously, the LA particles had already been used as uptake control in human umbilical vein endothelial cells as described by Matuszak et al. [19].

Flow cytometry measurements indicated that LA particles impaired cell growth even at low concentrations, but up to an iron concentration of 50 µg/mL there was no increase in the number of apoptotic and necrotic cells (Fig. 4A, Supplementary Data S2A).

The *in situ* synthesis improved the physicochemical properties of the particles, but the effects on the cells remained the same because the surface coating was still composed of lauric acid. LA(*in situ*) also impaired cell growth at low concentrations and led to an increased number of apoptotic and necrotic cells at concentrations above 50 µg/mL (Fig. 4B, S2B).

As shown by Poller et al. [20], lauric acid coated SPIONs are not colloidally stable in cell culture medium unless it is supplemented with FCS which builds a protein corona around the nanoparticles [21,22]. For this reason and to enhance the biocompatibility, LA(*in situ*) was coated with bovine serum albumin as previously discussed and performed by Zaloga et al. [15,23]. Due to the expected improved biocompatibility of LABSA particles, the viability experiments were performed up to a maximum iron concentration of 400 µg/mL. Although low concentrations limit cell proliferation, there are not more apoptotic and necrotic cells. From 100 µg/mL there is a slight increase in apoptotic and necrotic cells, but the percentage of viable cells only falls below 70% at 400 µg/mL (Fig. 4C, S2C).

To increase the uptake of LABSA particles, the BSA shell was aminated with ethylenediamine. In contrast to the negative zeta potential of the protein coating, amination produces a positive surface charge by adding primary amino groups, which should lead to an increased particle uptake through improved interaction with the negatively charged cell membrane [24]. Due to the potentially higher cytotoxicity of cationic nanoparticles [25], two different degrees of amination were tested.

As a precaution for the expected higher toxicity of the aminated particles, the experiments were carried out at concentrations of 10–100 µg/mL.

$LABSANH_2$low showed a slight increase in toxicity compared to LABSA and a negative effect on cell growth even at 25 µg/mL (Fig. 4D, S2D).

High aminated $LABSANH_2$ were tested simultaneously with the low aminated at the same iron concentrations. Every tested concentration led to an increase of the number of necrotic cells and impaired growth of cells (Fig. 4E, S2E).

3.3. Uptake

For magnetization of cells and targeting by magnetic fields the uptake of nanoparticles by cells or adhesion to cells is necessary. We speculated that high uptake rates lead to toxicity in the cells, thus, we had to find conditions with acceptable toxicity and relatively high SPION uptake and/or adhesion to cells at the same time. Parallel to the evaluation of biocompatibility by AxV/PI staining in flow cytometry we analyzed side scatter values of viable cells (Hoe + and DiI+), which indicates nanoparticle uptake. To estimate whether the particles are absorbed or adsorbed, a staining with Lucifer Yellow was performed. As can be seen in Supplementary Data S3, fluorescence increases for all particles after 24 h of incubation, which indicates that the particles are incorporated into the cells.

Analyzing the side scatter values we found that the higher the concentration of SPIONs the higher were the side scatter values. After incubating all SPION concentrations for 24 and 48 h, LA and LA(*in situ*) particles achieved higher SSc values after 48 h of incubation, LABSA and $LABSANH_2$low had similar values at 24 and 48 h and $LABSANH_2$high got higher side scatter values after 24 h (Fig. 5A–E).

Based on the side scatter data we selected conditions for the determination of cellular iron content by AES. LA and LA(*in situ*) nanoparticles were tested from 25 to 100 µg/mL with an incubation time of 24 and 48 h. 100 µg/mL served as a positive control as it was too toxic for further application but achieved high intracellular iron contents. When incubated with 50 µg/mL, LA particles achieved a maximum SPION uptake of 0.8 pg iron per cell after incubation for 24 h (Fig. 6A), LA(*in situ*) 0.65 pg iron per cell (Fig. 6B).

LABSA was used up to an iron concentration of 200 µg/mL which served as positive control, decreasing cell proliferation too much for further application. After 24 h of incubation with 100 µg/mL, a maximum uptake of 0.65 pg iron could be achieved (Fig. 6C). Consequently,

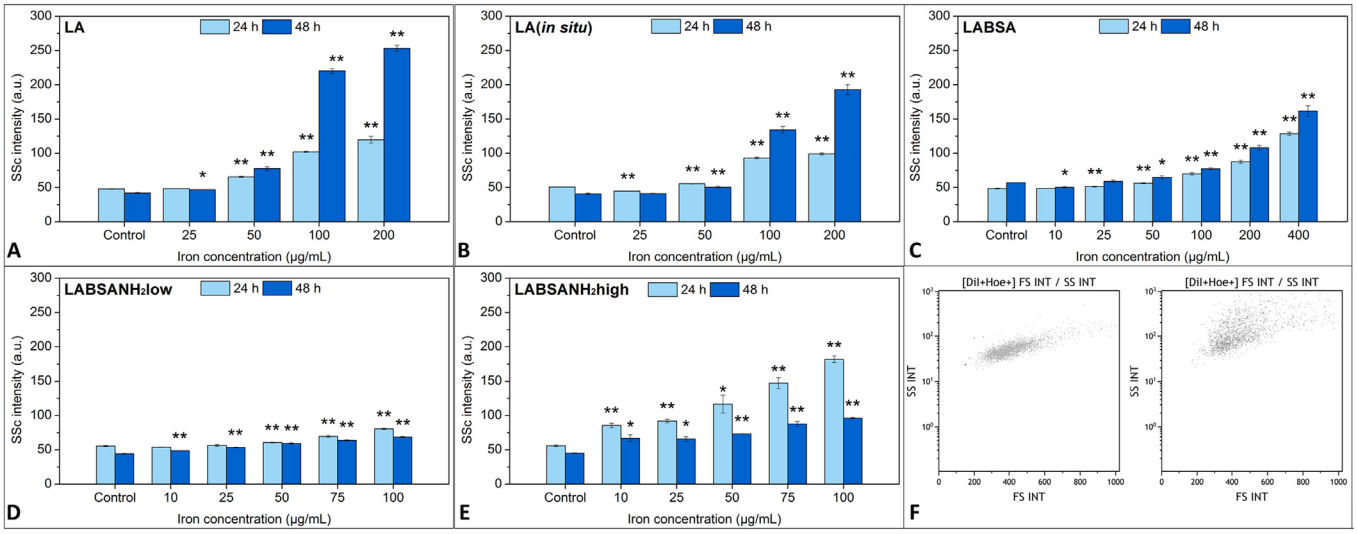

Fig. 5. Side scatter increase indicates cellular SPION uptake. A-E: Cellular granularity of viable cells after incubation with SPIONs. SSc increase was determined in flow cytometry and provides information about cellular granularity, which can be used to estimate the SPION uptake into cells or attachment to cells. Shown are the mean values with standard deviations. F: Flow cytometry raw data files of control cells (left) and cells treated with 50 µg/mL LABSANH$_2$high (right) after 24 h of incubation. For determination of SSc increase we gated on Hoechst positive events and viable cells (DiI +) only. All experiments shown in this figure were performed with cell line BW5147.3. Student's *t*-test compared to control: $^{*}p < 0.05$, $^{**}p < 0.005$.

compared to LA(*in situ*), the same absorption rate can be obtained using a higher concentration due to the improved biocompatibility.

Since the aminated SPIONs were not colloidally stable in cell culture medium, it was not yet possible to separate the incubated, loaded suspension cells from excess free particles by centrifugation.

For this reason, the iron uptake into the cells could not be measured directly by AES. Thus, uptake and/or attachment could only be estimated using the side scatter values (Fig. 5D + E).

Low amination degree did not lead to a significantly increased uptake rate compared to LABSA. As shown by the zeta potential measurements, the amount of amino groups was not yet sufficient to completely compensate for the negative charge of the albumin. With LABSANH$_2$high, on the other hand, side scatter values up to twice as high could be achieved, which suggested an increase in particle uptake and confirmed the assumption that a positive surface charge has an enhancing effect on the uptake of particles.

3.4. Magnetizability

To check the magnetizability of the loaded cells, videos were made with the same iron concentrations as used for the uptake experiments employing an inverse microscope. When a magnet was placed directly in the well, the cells moved towards the magnet and accumulated on its surface (Fig. 7, Supplementary Data Video 1: magnet was above the filmed area). If a magnet was placed in the adjacent well, the attraction was not as strong and only a part of the cells moved in the direction of the magnet (Supplementary Data Video 2: magnet was in the well to the right). The number of attracted cells and their speed increased with rising iron concentration (Supplementary Data S4). Velocity of fast moving cells was measured using the software "Tracker Video Analysis and Modeling Tool". In all recorded videos, there were cells that did not move. There are several reasons for this: the loading of the cells is not homogeneous due to the long incubation time with strongly proliferating cells, so that there are cells with more and cells with less internalized SPIONs.

In addition, these are suspension cells that have been filmed with an inverse microscope. It is only possible to focus many cells at once close to the bottom of the well. In contrast to adherent cells, cells sedimented on the bottom do not adhere to the plastic surface, but the magnetic attraction must first overcome adhesive and frictional forces.

With concentrations of 25 and 50 µg/mL LA and LA(*in situ*) cells were attractable by the magnet. However, due to the high toxicity of these particles, their future use with primary cells does not seem reasonable. With LABSA particles at 100 µg/mL it was also possible to attract loaded cells with a magnet in the same well as in a neighboring well. Due to their lack of colloidal stability in cell culture media, LABSANH$_2$ could not be tested yet.

4. Conclusions

Many SPION systems used to track T lymphocytes in MRI can be found in the literature, but provide no information about the

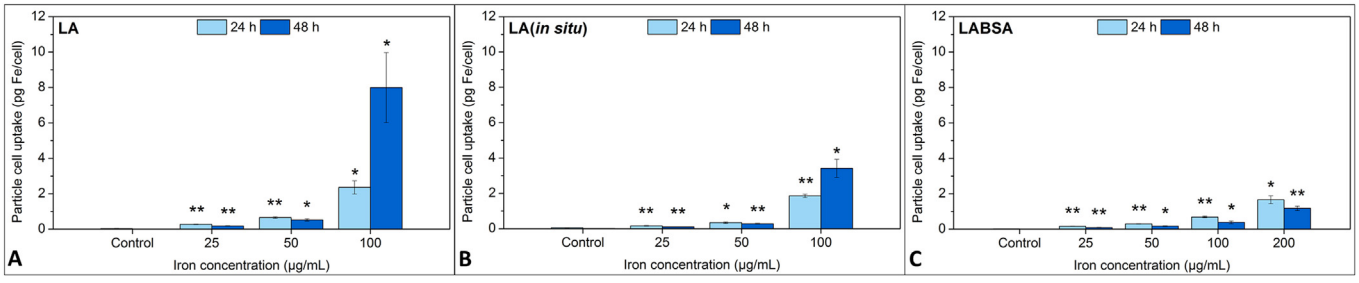

Fig. 6. Intracellular iron content. A–C: The intracellular iron content in pg per cell was determined by atomic emission spectroscopy. The highest nanoparticle concentration each served as positive control. Shown are the mean values with standard deviations. All experiments shown in this figure were performed with cell line BW5147.3. Student's *t*-test compared to control: $^{*}p < 0.05$, $^{**}p < 0.005$.

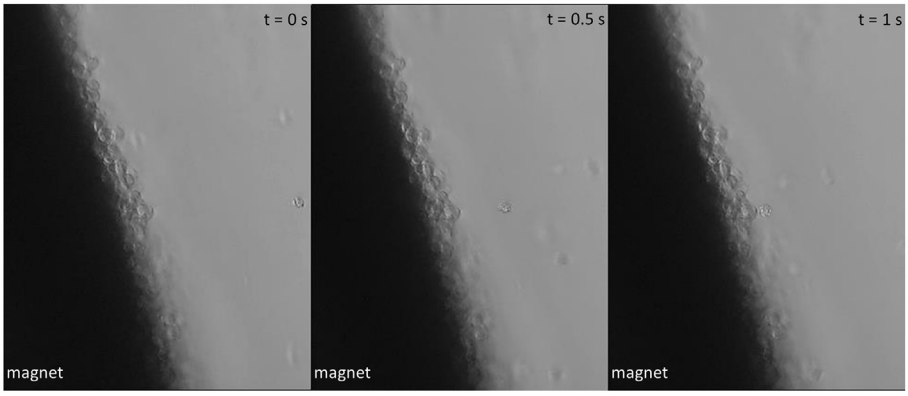

Fig. 7. Magnetic attraction of SPION-loaded T cells. A small cylindrical magnet (8 mm × 5 mm, approx. 50 mT) was placed in a well with LA (*in situ*) bearing T cells and filmed. Cells moved towards the magnet's surface and accumulated there. (Colors and contrast have been adjusted for enhanced visualization.) (For interpretation of the references to colour in this figure legend, the reader is referred to the web version of this article.)

magnetizability of the SPIONs used and the loaded cells. However, moving T cells to a specific location by means of an external magnetic field is a new and innovative method. Our results prove the concept of magnetic T cell targeting in vitro, analogous to magnetic drug targeting. Although targeting requires high SPION concentrations with sufficient susceptibility in the cells in contrast to tracking, we have succeeded in recording first videos in which T cells loaded with SPIONs are attracted by magnets.

Most promising combinations for the investigated cell lines until now are LABSA 100 µg/mL incubated for 24 h and LABSANH_2high 10 µg/mL incubated for 24 h.

5. Outlook

The challenge and next task will be to develop a particle system that has the ideal balance between toxicity and cellular uptake. It should be colloidally stable in cell culture medium or taken up from protein-free buffer solutions in less than one hour to maintain cell viability. In addition, it is important to establish a method for the separation of loaded cells and excess unstable particles.

Another approach is not to bring the particles into the cells, but to attach nanoparticles to the cell surface. However, it must be taken into consideration that the particles must not trigger any immune reactions and do not block any receptors relevant for the function of the T cells.

Funding

This study was supported by the Emerging Fields Initiative BIGTHERA of the Friedrich-Alexander-Universität Erlangen-Nürnberg (FAU) and the Manfred-Roth-Stiftung, Fürth, Germany.

Declarations of interest

None.

Appendix A. Supplementary data

Supplementary data to this article can be found online at https://doi.org/10.1016/j.jmmm.2018.10.022.

References

[1] World Health Organization Regional Office for Europe. Cancer – Data and statistics. 2018 [cited 2018 17.08.]; Available from: http://www.euro.who.int/en/health-topics/noncommunicable-diseases/cancer/data-and-statistics.
[2] S.E. Church, J. Galon, Tumor microenvironment and immunotherapy: the whole picture is better than a glimpse, Immunity 43 (4) (2015) 631–633.
[3] C. Denkert, et al., Standardized evaluation of tumor-infiltrating lymphocytes in breast cancer: results of the ring studies of the international immuno-oncology biomarker working group, Mod. Pathol. 29 (10) (2016) 1155–1164.
[4] J. Galon, et al., Type, density, and location of immune cells within human colorectal tumors predict clinical outcome, Science 313 (5795) (2006) 1960–1964.
[5] S.R. Frankel, P.A. Baeuerle, Targeting T cells to tumor cells using bispecific antibodies, Curr. Opin. Chem. Biol. 17 (3) (2013) 385–392.
[6] V. Vanecek, et al., Highly efficient magnetic targeting of mesenchymal stem cells in spinal cord injury, Int. J. Nanomed. 7 (2012) 3719–3730.
[7] R. Tietze, et al., Magnetic nanoparticle-based drug delivery for cancer therapy, Biochem. Biophys. Res. Commun. 468 (3) (2015) 463–470.
[8] C. Janko, et al., Magnetic drug targeting reduces the chemotherapeutic burden on circulating leukocytes, Int. J. Mol. Sci. 14 (4) (2013) 7341–7355.
[9] R. Tietze, et al., Visualization of superparamagnetic nanoparticles in vascular tissue using XmuCT and histology, Histochem. Cell Biol. 135 (2) (2011) 153–158.
[10] H. Unterweger, et al., Dextran-coated superparamagnetic iron oxide nanoparticles for magnetic resonance imaging: evaluation of size-dependent imaging properties, storage stability and safety, Int J Nanomed. 13 (2018) 1899–1915.
[11] O. Brunke, et al., Determination of the magnetic particle distribution in tumour tissue by means of X-ray tomography, J. Phys.: Conden. Matter. 18 (2006).
[12] A.J. Beer, et al., Visualization of antigen-specific human cytotoxic T lymphocytes labeled with superparamagnetic iron-oxide particles, Eur. Radiol. 18 (6) (2008) 1087–1095.
[13] L. Liu, et al., Tracking T-cells in vivo with a new nano-sized MRI contrast agent, Nanomedicine 8 (8) (2012) 1345–1354.
[14] R. Tietze, et al., Efficient drug-delivery using magnetic nanoparticles–biodistribution and therapeutic effects in tumor bearing rabbits, Nanomedicine 9 (7) (2013) 961–971.
[15] J. Zaloga, et al., Development of a lauric acid/albumin hybrid iron oxide nanoparticle system with improved biocompatibility, Int. J. Nanomed. 9 (2014) 4847–4866.
[16] N. Nakajima, Y. Ikada, Mechanism of amide formation by carbodiimide for bioconjugation in aqueous media, Bioconjug. Chem. 6 (1) (1995) 123–130.
[17] R.P. Friedrich, et al., Flow cytometry for intracellular SPION quantification: specificity and sensitivity in comparison with spectroscopic methods, Int. J. Nanomed. 10 (2015) 4185–4201.
[18] P.J. Lamothe, P.G. McCormick, Role of hydrindantin in the determination of amino acids using ninhydrin, Anal. Chem. 45 (11) (1973) 1906–1911.
[19] J. Matuszak, et al., Shell matters: Magnetic targeting of SPIONs and in vitro effects on endothelial and monocytic cell function, Clin. Hemorheol. Microcirc. 61 (2) (2015) 259–277.
[20] J.M. Poller, et al., Selection of potential iron oxide nanoparticles for breast cancer treatment based on in vitro cytotoxicity and cellular uptake, Int. J. Nanomed. 12 (2017) 3207–3220.
[21] J.S. Gebauer, et al., Impact of the nanoparticle-protein corona on colloidal stability and protein structure, Langmuir 28 (25) (2012) 9673–9679.
[22] A. Lesniak, et al., Effects of the presence or absence of a protein corona on silica nanoparticle uptake and impact on cells, ACS Nano 6 (7) (2012) 5845–5857.
[23] D.S. Goodman, The interaction of human serum albumin with long-chain fatty acid anions, J. Am. Chem. Soc. 80 (15) (1958) 3892–3898.
[24] J. Lin, A. Alexander-Katz, Cell membranes open "doors" for cationic nanoparticles/biomolecules: insights into uptake kinetics, ACS Nano 7 (12) (2013) 10799–10808.
[25] E. Fröhlich, The role of surface charge in cellular uptake and cytotoxicity of medical nanoparticles, Int. J. Nanomed. 7 (2012) 5577–5591.